

# Tunable Light Emission from Lignin: Various Photoluminescence Properties Controlled by the Lignocellulosic Species, Extraction Method, Solvent, and Polymer

Masatsugu Takada,\* Yutaka Okazaki,\* Haruo Kawamoto, and Takashi Sagawa



Cite This: *ACS Omega* 2022, 7, 5096–5103



Read Online

ACCESS |



Metrics & More



Article Recommendations



Supporting Information

**ABSTRACT:** This report describes the tunable light emission from lignin, which was achieved by carefully selecting the lignocellulosic species, extraction method, solvent, and polymer. Lignins comprising various taxonomic species with distinct primary structures exhibited diverse photoluminescence (PL) intensities and spectral patterns. Investigations probing how the solvent affects the PL properties revealed that the PL quenching phenomenon originated from the decreasing distance between aromatic moieties (luminophores). Therefore, polymers can play key roles as media to modulate the distance between luminophores, and the PL intensity can be enhanced by employing a relatively stiff polymer. In terms of the emission color, the PL spectral pattern can be tuned by changing the lignin primary structures or by deprotonating the phenolic hydroxyl groups. By modulating these influencing factors, various light emissions were obtained from lignins in solutions and transparent solid materials.



## INTRODUCTION

Lignocellulosic materials are sustainable and renewable feedstocks that have the potential to replace nonsustainable, fossil-derived raw materials, such as fuels and other chemicals. The cell walls of lignocellulosic materials are predominantly composed of cellulose, hemicellulose, and lignin; the latter two polysaccharide components account for 60–70% of the material that can be used as a feedstock for various chemicals and substances, such as pulp and cellulose nanofibers. In contrast, lignin, which is the most abundant natural aromatic polymer in the world, is difficult to utilize owing to its heterogeneous and complex structure. In general, lignin is produced as a byproduct in the fabrication of Kraft pulp or sulfite pulp, during which, the produced lignin is burned to provide heat energy. In addition to heat generation, commercial lignin can be used as a dispersant, a binder, or an emulsifier.<sup>1</sup> Notably, lignin has a large molar extinction coefficient, which indicates that it has the potential to serve as an optical material. For example, in one case, lignin was added to a polymer as an ultraviolet (UV) absorber.<sup>2,3</sup> Recently, fluorescence microscopy has been employed to examine the distribution of lignin within the cell walls of pretreated biomass by exploiting its autofluorescence properties.<sup>4–6</sup> Additionally, a lignin-based fluorescence sensor has been developed.<sup>7,8</sup> However, lignin is not commonly used as a feedstock for luminescent materials, possibly because of its complex photoluminescence (PL) mechanism. For example, some research groups proposed that aggregation-induced emission (AIE) is the main mechanism of lignin PL.<sup>9–11</sup> However, the lignin PL was not observed in the solid state (e.g., lignin

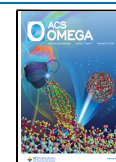
powder and cardboard), indicating that the PL mechanism obviously cannot be explained only by AIE. Furthermore, some studies have used lignin model compounds to determine the origin of its fluorescence properties; a coniferyl alcohol anion,<sup>12</sup> a stilbene structure,<sup>13,14</sup> a phenylcoumarone structure,<sup>15</sup> and a dibenzodioxocin structure<sup>14</sup> have all been considered as potential candidates for such a chromophore. Radotić et al. analyzed the fluorescence properties of a lignin model (a dehydrogenated polymer) based on deconvoluted emission spectra and time-resolved decay-associated excitation/emission spectra, and they confirmed the existence of distinct fluorophores in the lignin model polymer.<sup>16</sup> However, even these simple model compounds exhibited complex fluorescence, and their spectra differed from those of natural lignin. These distinctions may have originated from several complex factors, such as the three-dimensional network structure, molecular weight, distance between luminophores within the lignin molecule, and solubility in the employed solvents.

To effectively use lignin as a luminescent material, it is necessary to control its luminescence properties, e.g., color and intensity. This work explored the influence of lignocellulosic

**Received:** October 31, 2021

**Accepted:** December 8, 2021

**Published:** January 31, 2022



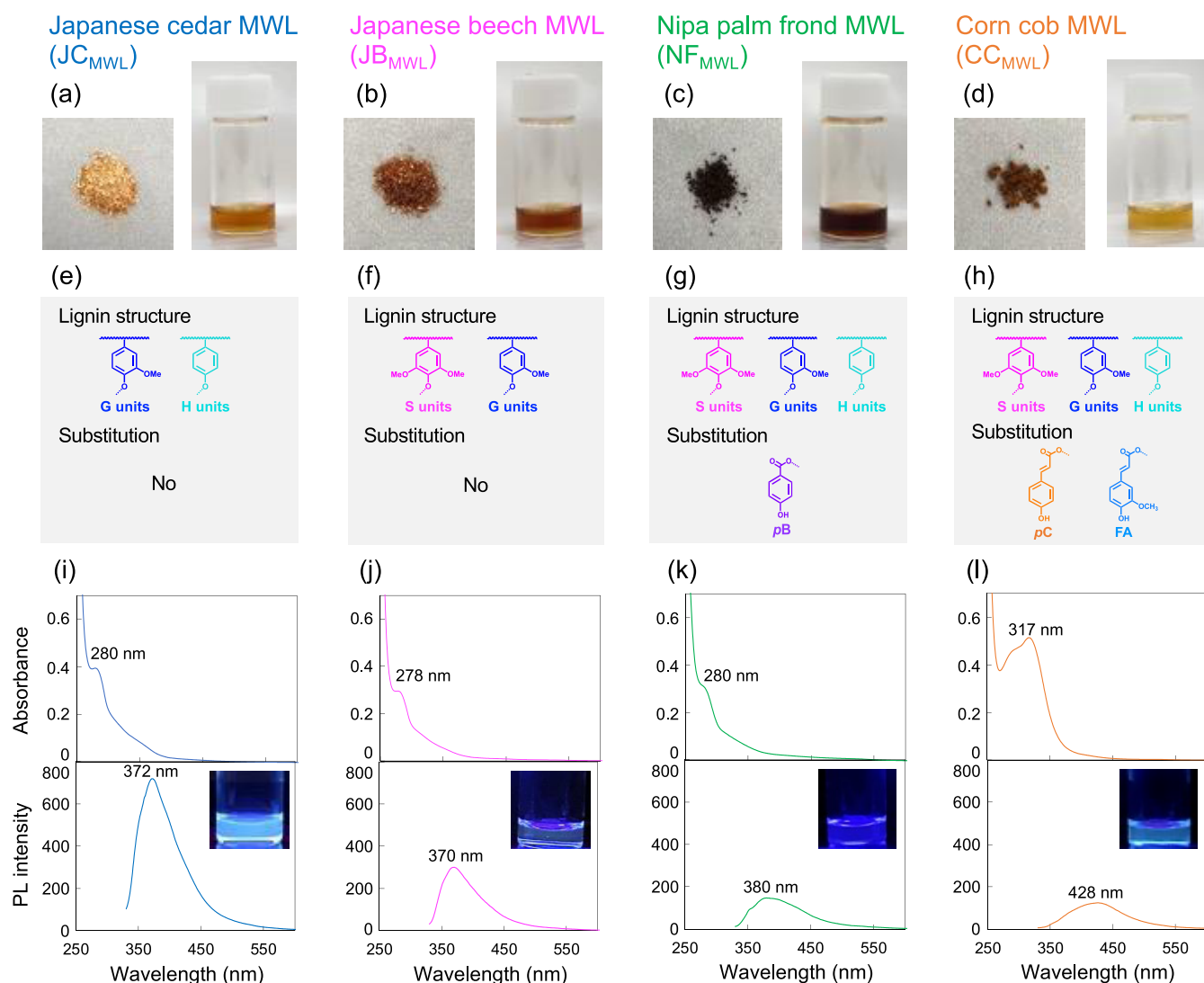


**Figure 1.** (a–d) Photos of milled wood lignins from four biomass species (JC<sub>MWL</sub>, JB<sub>MWL</sub>, NF<sub>MWL</sub>, and CC<sub>MWL</sub>, respectively) before (left) and after (right) dissolving in DMSO (10 mg mL<sup>-1</sup>). (e–h) Corresponding lignin components and substituent structures detected by 2D-NMR. (i–l) Corresponding UV–vis absorption (top) and PL spectra (bottom) in dilute DMSO solutions (0.1 mg mL<sup>-1</sup>) excited at 320 nm. Insets show photos captured under UV light at 365 nm. S unit = syringyl; G unit = guaiacyl; H unit = *p*-hydroxyphenylpropane; pB = *p*-hydroxybenzoate; pC = *p*-coumaric acetate; FA = ferulic acetate.

species, extraction methods, solvents, and polymers on the PL properties of the products.

This study involved the preparation of milled wood lignin (MWL), which is considered to be the original lignin structure, from four taxonomical species: a gymnosperm softwood (Japanese cedar; JC), an angiosperm dicotyledons hardwood (Japanese beech; JB), an angiosperm monocotyledons Aceraceae (nipa palm frond; NF), and an angiosperm monocotyledons Poaceae (corn cob; CC). The various lignins were prepared via five extraction techniques (MWL, alkali, Kraft, organosolv, and sulfite treatments), which represent common delignification methods used in the pulp and paper industry. Then, the PL properties of the prepared lignins were analyzed to evaluate the effects of structural differences on the resulting PL. Furthermore, various solvents and polymers were used to understand the impacts of the environmental media on the PL properties.

## MATERIALS AND METHODS

**Materials and Chemicals.** The lignocellulosic sources included sapwood of Japanese cedar (JC), sapwood of Japanese beech (JB), nipa palm frond (NF), and corn cob (CC). Detailed information for these lignocellulosics is provided in Table S1. The lignocellulosic biomass materials were milled in a Wiley mill (Thomas Scientific, NJ), and the obtained MWL flour was sieved with mesh screens to collect particles between 0.15 and 1.0 mm. The sieved flour was extracted with acetone in a Soxhlet apparatus and dried at 105 °C for 24 h prior to the experiments. Poly(2-hydroxyethyl methacrylate) (PHEMA; average  $M_w$ : ~15 000, ~120 000, ~350 000) and poly(methyl methacrylate) (PMMA; average  $M_w$ : ~300 000) were purchased from Sigma-Aldrich Co. LLC. All chemicals used in this study were of reagent grade, purchased from Nacalai Tesque, Inc. (Kyoto, Japan), and used without further purification.

**Preparation of Lignins.** The MWL samples were prepared from four wood species according to the method

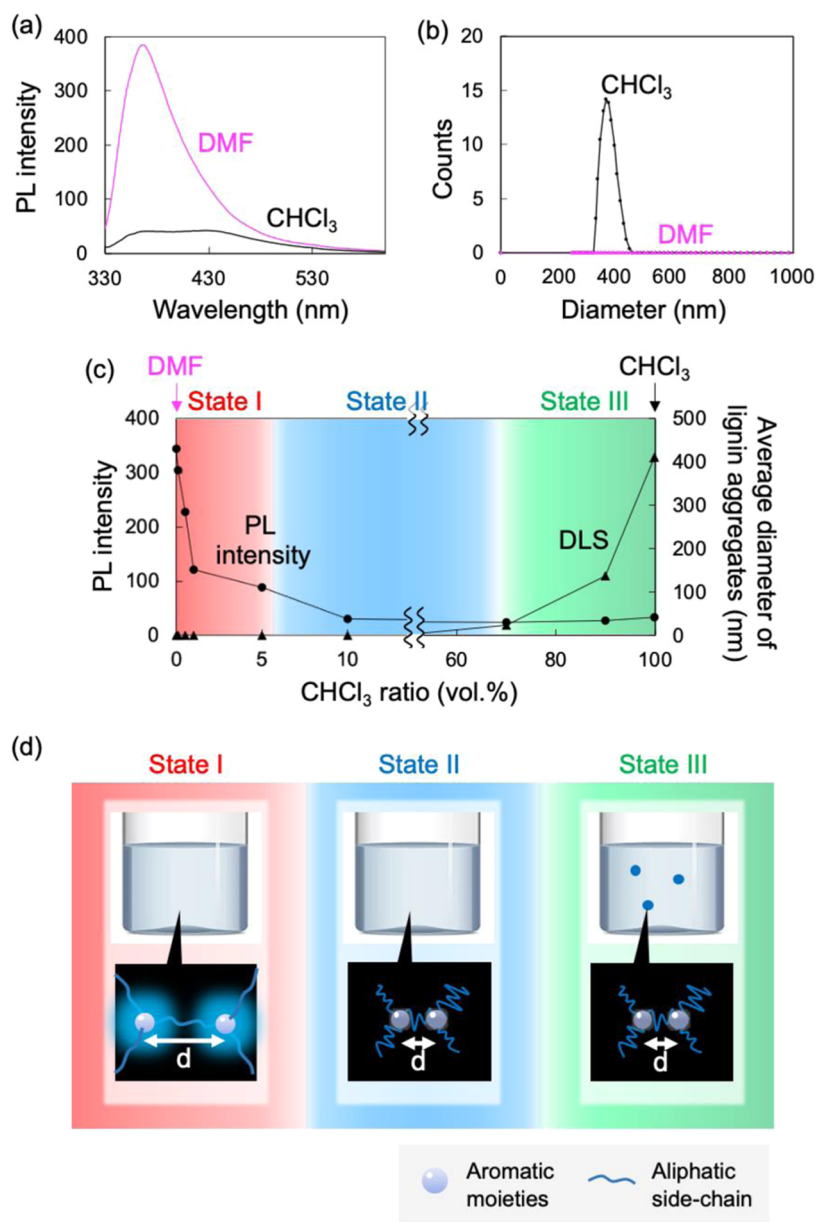


**Figure 2.** (a) PL spectra of  $\text{JB}_{\text{MWL}}$  in DMF and  $\text{CHCl}_3$  excited at 320 nm ( $10 \text{ mg mL}^{-1}$ ). (b) Average diameter of lignin aggregates detected by DLS. (c) PL intensity and average diameter detected by DLS as a function of the  $\text{CHCl}_3$  concentration in DMF/ $\text{CHCl}_3$  mixtures. (d) Schematic diagrams depicting quenching and aggregate formation.

described by Björkman (1956).<sup>17</sup> The extractive-free flour was milled for 48 h in a vibratory ball mill VS-1 (Irie Shokai Co., Ltd., Tokyo, Japan). The applied extraction methods, i.e., alkali (soda), Kraft, organosolv, and sulfite treatments, were performed via adapted simplified methods.<sup>1</sup> Briefly, extractive-free beech flour and treatment chemicals were placed in a 5.0 mL reaction vessel made of Inconel-625. The vessel was sealed and immersed in a molten salt bath, which was preheated to a designated temperature. After an adequate reaction time, the reaction was quenched in a water bath. The chemical reagents, treatment temperatures, and times for each extraction method are as follows: alkali, NaOH, 170 °C for 1 h; Kraft, NaOH, and  $\text{Na}_2\text{S}$ , 170 °C for 1 h; organosolv, ethanol, 210 °C for 5 min; sulfite, NaOH, and  $\text{Na}_2\text{SO}_3$ , 160 °C for 1 h. For the alkali, Kraft, and organosolv treatments, the soluble portion was concentrated by vacuum evaporation, and the product was precipitated into a dilute acid solution to purify

the lignin. The obtained alkali lignin (AL), Kraft lignin (KL), and organosolv lignin (OL) were then washed with ultrapure water. For the sulfite lignin (SL), precipitation did not occur because of its hydrophilic structure. Therefore, the concentrated portion obtained following vacuum evaporation was used for further experiments.

To prepare samples for two-dimensional nuclear magnetic resonance spectroscopy (2D-NMR; Bruker AC-400, 400 MHz, Bruker Corp., MA), i.e., heteronuclear single quantum coherence (HSQC) characterization experiments, approximately 100 mg of each sample was dissolved in deuterated dimethylsulfoxide ( $\text{DMSO-}d_6$ ) (700  $\mu\text{L}$ ).

**Ultraviolet–Visible (UV–Vis) Absorption and Photoluminescence (PL) Spectroscopy.** The prepared lignins were dissolved in nine solvents (at  $0.1 \text{ mg mL}^{-1}$  concentrations): DMSO, *N,N*-dimethylformamide (DMF), acetonitrile, ethyl glycol, methanol, ethanol, ethyl acetate, chloroform

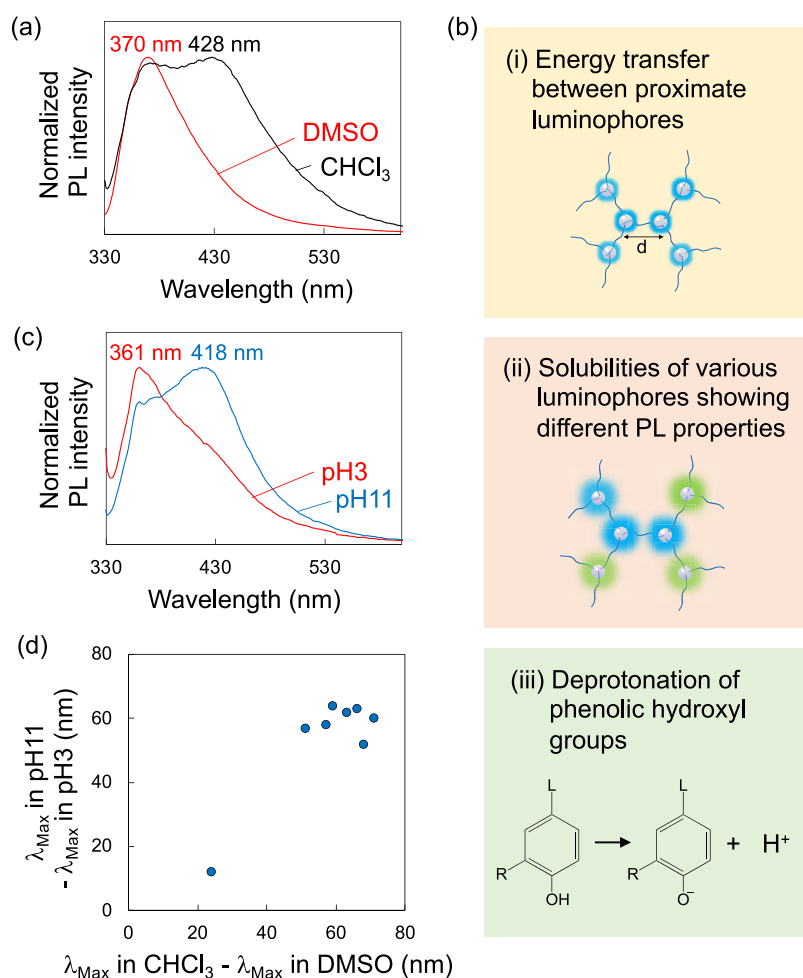


**Figure 3.** (a) Normalized PL spectra of  $\text{JB}_{\text{MWL}}$  in DMSO and  $\text{CHCl}_3$  excited at 320 nm. (b) Three possible mechanisms leading to peak appearance in  $\text{CHCl}_3$ . (c) Normalized PL spectra of  $\text{JB}_{\text{MWL}}$  in aqueous solutions excited at 320 nm. (d) Differences in peak positions in DMSO and  $\text{CHCl}_3$  versus differences in peak positions under alkaline and acidic conditions.

( $\text{CHCl}_3$ ), and toluene. Their UV–vis absorption and PL spectra were recorded with V-650 (Jasco Co., Ltd., Tokyo, Japan) and FP-8600 (Jasco Co., Ltd., Tokyo, Japan) instruments, respectively. For the analysis of aqueous solutions, acidic (pH = 3) and alkaline (pH = 11) solutions were prepared using hydrochloric acid and sodium hydroxide, respectively. The prepared lignins were dissolved in these aqueous solutions at concentrations of 0.1 mg  $\text{mL}^{-1}$ .

**Characterization of Lignin Aggregation.** Lignin aggregates in DMF and chloroform solutions were evaluated by a dynamic light scattering (DLS) method using a  $\zeta$ -potential and a particle size analyzer (ELSZ2000ZS; Otsuka Electronics Co., Ltd., Osaka, Japan). In addition, each solution was cast onto a glass coverslip and dried in air for 1 week to remove the solvent prior to conducting scanning electron microscopy (SEM) and Fourier transform infrared (FT-IR) spectroscopy analysis. SEM observations were performed using an SU-6600 instrument (Hitachi High-Technologies Corporation, Tokyo, Japan). Samples were placed on an SEM stub, coated in gold, and then analyzed at an accelerating voltage of 5 kV. FT-IR spectra were recorded in the attenuated total reflectance (ATR) mode (IRAffinity-1S instrument, Shimadzu Co., Kyoto, Japan).

**Preparation of Lignin-Containing Transparent Films.** PHEMA was dissolved in DMF at a concentration of 100 mg

$\text{mL}^{-1}$ , and PMMA was dissolved in DMF or chloroform at 100 mg  $\text{mL}^{-1}$ . Then, 1 mL of the desired polymer solution was mixed with 10  $\mu\text{L}$  of various lignins dissolved in DMSO at 10 mg  $\text{mL}^{-1}$ . The mixtures were cast onto quartz slides and dried under air to obtain lignin-containing transparent films.

## RESULTS AND DISCUSSION

**PL Spectra of Four MWLs in Various Solvents.** The powdered samples of four types of MWLs prepared from four taxonomical species (denoted  $\text{JC}_{\text{MWL}}$ ,  $\text{JB}_{\text{MWL}}$ ,  $\text{NF}_{\text{MWL}}$  and  $\text{CC}_{\text{MWL}}$ ) appeared light brownish, brownish, dark brownish, and brownish in color, respectively (Figure 1a–d). Although these powders did not exhibit significant light emission, when they were dissolved in DMSO or DMF, all of the obtained solutions exhibited clear PL with slightly different colors and light intensities (insets of Figure 1i–l). These differences in absorption and luminescence were quantitatively evaluated by UV–vis and PL spectroscopies. In the case of  $\text{JC}_{\text{MWL}}$ , an absorption peak was observed at 280 nm, and when the solution was excited with 320 nm light, clear PL with a peak at 372 nm was observed (Figure 1i). The  $\text{JB}_{\text{MWL}}$  and  $\text{NF}_{\text{MWL}}$  samples showed similar absorption and PL, with weak emission intensities (Figure 1j,k). In contrast,  $\text{CC}_{\text{MWL}}$  exhibited a significantly different absorption peak at 317 nm and a PL peak at 428 nm (Figure 1l). Based on HSQC 2D-NMR analysis of

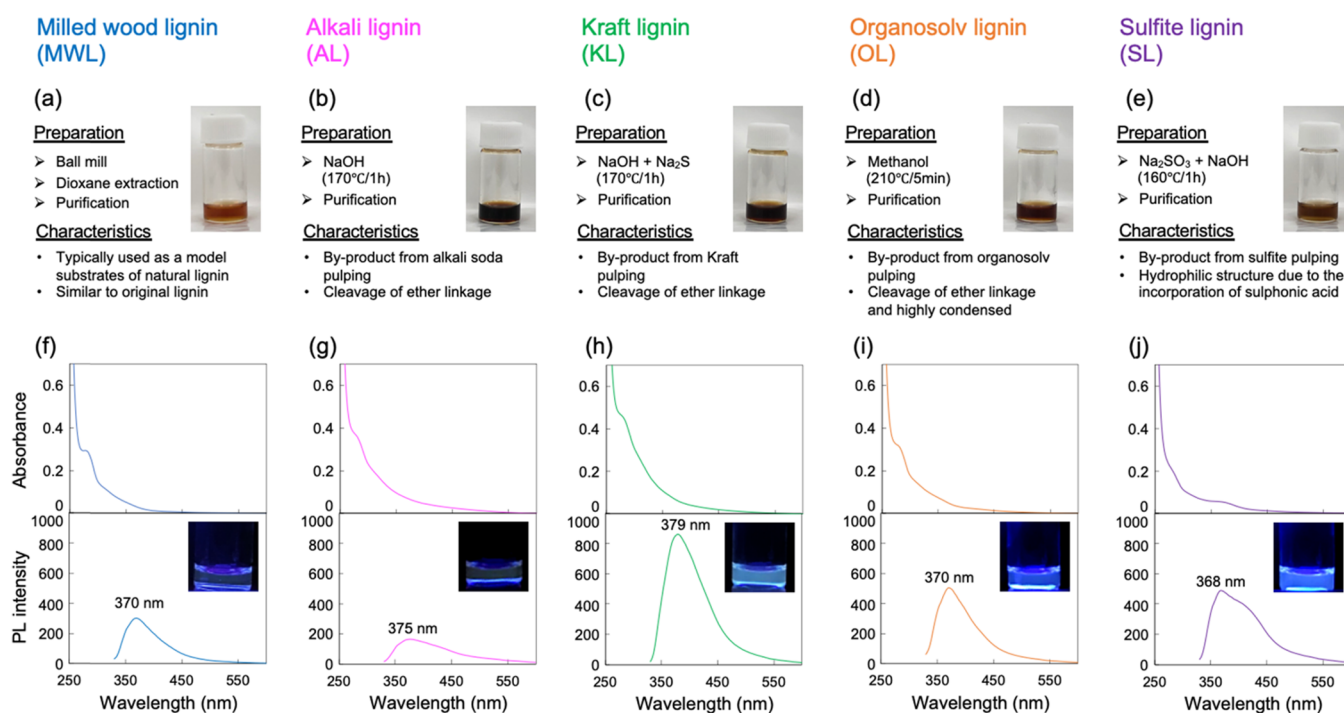


**Figure 4.** (a–e) Photos of the five prepared lignins (MWL, AL, KL, OL, and SL, respectively) from Japanese beech in DMSO ( $10 \text{ mg mL}^{-1}$ ). (f–j) UV–vis absorption (top) and photoluminescence spectra (bottom) of the corresponding lignins in dilute DMSO solutions ( $0.1 \text{ mg mL}^{-1}$ ) excited at 320 nm. Insets show pictures captured under UV light at 365 nm.

these lignins (Figure S1), the differences in the positions of the absorption and PL peaks likely resulted from the different aromatic moieties and aliphatic side-chain structures in the materials (Figure 1e–h). For example,  $\text{CC}_{\text{MWL}}$  contained the cinnamate structure such as *p*-coumarate and ferulate, which extended the  $\pi$ -conjugated system, resulting in the absorption and PL peaks at a longer wavelength.

Light emission from lignin can also be tuned by the external environment, which can be controlled somewhat by modulating the solvent's properties. To study the effect of the solvent on the PL exhibited by the lignins, nine solvents spanning a range of properties were selected; the obtained UV–vis and PL spectra excited at 280 and 320 nm are shown in Figures S2–S5. Solutions of the  $\text{JC}_{\text{MWL}}$ ,  $\text{JB}_{\text{MWL}}$ , and  $\text{NF}_{\text{MWL}}$  lignins in hydrophilic solvents (e.g., DMSO, DMF) had higher PL intensities than in hydrophobic solvents (e.g., ethyl acetate,  $\text{CHCl}_3$ ). In particular, lignin solutions in  $\text{CHCl}_3$  showed completely unique PL spectra, with low intensity (i.e., quenching) and a new peak at 430 nm.

**Mechanistic Studies of Quenching and Peak Appearance in  $\text{CHCl}_3$ .** It is important to understand the mechanism(s) governing the quenching process and the appearance of peaks to control the PL intensity and color, respectively. To explore the quenching phenomenon,  $\text{JB}_{\text{MWL}}$  solutions were prepared in DMF and  $\text{CHCl}_3$ , and these solutions had completely different PL intensities (Figure 2a). As shown in Figure S3, there is a positive correlation between the dielectric constant of the solvent and the PL intensity of  $\text{JB}_{\text{MWL}}$  solutions. The clear distinction between hydrophilic and hydrophobic solvents was caused by the formation of aggregates; after standing under ambient conditions, some aggregation was observed only in hydrophobic solvents.

As the standing time continued, the PL spectra of the  $\text{CHCl}_3$  solutions changed (Figure S6). However, once the mixture was

stirred, the PL spectrum returned to the original profile, thus indicating that the aggregates were formed via weak intermolecular interactions rather than through strong covalent bonds. Figure S7a shows that such aggregates were clearly generated in highly concentrated solutions of  $\text{JB}_{\text{MWL}}$  in  $\text{CHCl}_3$ , ultimately resulting in the formation of visible precipitates; no aggregation was observed in the DMF solution, even at the same concentration. Both of these solutions were cast on glass coverslips and dried under air to remove the solvent. According to SEM observations of the dried lignins, globular aggregates with diameters between 10 and 50  $\mu\text{m}$  were observed only in the dried lignin from the  $\text{CHCl}_3$  solution, but not in that obtained from the DMF solution (Figure S7a). When these solutions were analyzed by dynamic light scattering (DLS), aggregates with diameters of dozens of micrometers were detected only in the  $\text{CHCl}_3$  solution (Figure S7b), indicating that lignin aggregates were formed in  $\text{CHCl}_3$ , but lignin remained completely dissolved in DMF. The dried lignins were also analyzed using FT-IR (Figure S7c). The peak at approximately  $1600 \text{ cm}^{-1}$ , which originates from the aromatic ring,<sup>18</sup> was slightly shifted in the sample prepared in  $\text{CHCl}_3$  relative to that prepared in DMF, despite the fact that they had identical compositions. This shift suggests that the vibrations of the aromatic region were suppressed by the aggregation. Figure 2c plots the PL intensity and average diameter versus the concentration of  $\text{CHCl}_3$  in DMF/ $\text{CHCl}_3$  mixtures. PL quenching was observed above 5 vol % of  $\text{CHCl}_3$ , although no aggregation was observed up to 70 vol % of  $\text{CHCl}_3$  (State II in Figure 2c). Based on these results, we concluded that the PL quenching occurred as a result of the decreasing distance between aromatic moieties (luminophores). A close proximity of luminophores leads to microscale aggregate formation, as illustrated in Figure 2d.

Three potential mechanisms were considered to explain the new peak observed in  $\text{CHCl}_3$  (Figure 3a): (i) energy transfer between proximal luminophores; (ii) differing solubilities of luminophores with different PL properties; and (iii) deprotonation of phenolic hydroxyl groups (Figure 3b).

In the first proposed mechanism involving energy transfer, the formation of aggregates in hydrophobic solvents disrupts each luminophore, thus inducing energy transfer to another luminophore, which could be detected as a difference in the PL lifetimes ( $\tau$ ). However, PL lifetime measurements revealed no significant difference between lignin in DMF ( $\tau = 2.53$  ns) versus in  $\text{CHCl}_3$  ( $\tau = 2.28$  ns), indicating that energy transfer is not the main mechanism causing longer wavelength PL in  $\text{CHCl}_3$ .

The second hypothesis is based on the consideration that the lignin macromolecules comprise various luminophores, which have different solubilities. Indeed, distinct PL peak positions were derived from luminophores having different primary structures (Figure 1e–h). If the solubility of a given luminophore is the main reason for a peak's appearance, a similar peak should be observed in a solvent having similar hydrophobicity (i.e., dielectric constant ( $\epsilon$ )). However, a comparison of the PL spectra of  $\text{JB}_{\text{MWL}}$  in  $\text{CHCl}_3$  ( $\epsilon = 4.81$ ) and diethyl ether ( $\epsilon = 4.34$ ), as shown in Figure S8, revealed that their spectral profiles were distinct, despite the fact that similar luminophores were dissolved in the two solvents. Therefore, it was concluded that although the second hypothesis may occur, another mechanism should be considered.

The third proposed mechanism involves the deprotonation of phenolic hydroxyl groups in  $\text{CHCl}_3$ . The peak profiles observed in aqueous solutions at high and low pHs (Figure 3c) were similar to those obtained in  $\text{CHCl}_3$  and DMSO, respectively. The PL spectrum recorded for the alkaline solution contained a peak at a longer wavelength than that in the acidic solution. Interestingly, the difference in the peak positions between alkaline and acidic solutions (418–361 nm = 57 nm) was close to the peak difference in DMSO versus  $\text{CHCl}_3$  solutions (428–370 nm = 58 nm). Similar behavior was observed in all lignins tested herein (Figure 3d; original data presented in Figures S9–S12 and S18–S21). These results indicated that the deprotonation of phenolic hydroxyl groups under alkaline conditions shifted the PL peak position to a longer wavelength; thus, a similar mechanism likely occurred in  $\text{CHCl}_3$ . In fact, the proton concentration in  $\text{CHCl}_3$  was higher than that in the other tested solvents (Figure S13), which supported this hypothesis. The deprotonation behavior of phenolic groups can also be detected by UV–vis spectroscopy (Figure S22, e.g., decrease at 280 nm and increase at 350 nm).

**Effect of Lignin Extraction Method on PL Spectra.** To elucidate how the extraction method influenced the lignin PL properties, five lignins (MWL, alkali lignin (AL), Kraft lignin (KL), organosolv lignin (OL), and sulfite lignin (SL)), which are the common lignin-based byproducts in the pulp and paper industry, were prepared from Japanese beech xylem. These lignin samples were dissolved in DMSO ( $0.1$  mg  $\text{mL}^{-1}$ ), and their UV–vis and PL spectra are shown in Figure 4. Similar to the MWLs shown in Figure 1, all tested lignins exhibited PL, and the UV–vis and PL spectra varied depending on the applied extraction method. For example, among the five lignins, KL had the highest PL intensity and a peak at a longer wavelength (379 nm).

To study the effect of the solvent on the PL properties of the lignins, their UV–vis and PL spectra were obtained in nine solvents after exciting at 280 and 320 nm (Figures S14–S17). Similar to the MWLs (Figures 2a and 3a), all five lignins experienced quenching and the appearance of a new peak in the  $\text{CHCl}_3$  solution. The PL intensity of the SL was quite low in hydrophobic solvents, such as  $\text{CHCl}_3$  and ethyl acetate (Figure S17). Considering that a sulfonate group was incorporated into the side chain of the lignin molecule following the sulfite pulping process, the solubility of SL in hydrophobic solvents was low relative to the other tested lignins, thus causing its relatively lower PL intensity. Furthermore, the KL results revealed a positive correlation between the PL intensity and the solvent viscosity (Figure S15). This relationship was also observed in lignins prepared by other extraction methods (Figures S14–S17), but KL showed the strongest correlation. This influence of solvent viscosity on the PL can be explained by the restriction of molecular motion.<sup>19</sup> During the KL pulping process, the dibenzodioxocin structure, which represents a major branching point of the wood lignin polymer network, is cleaved more efficiently than in other pulping methods.<sup>20</sup> Therefore, its less-branched structure would be highly affected by the solvent's viscosity.

Given that all five lignins were prepared from the same starting material, the observed range of PL properties likely originated from the differences in the lignin primary structures (i.e., aromatic moieties and functional groups) and highly ordered structures (i.e., molecular weight distribution and linkages between aromatic moieties) formed during each extraction procedure. The solution environment clearly influenced the PL properties, and therefore this knowledge was then applied to solid-state, polymeric media.

**PL Spectra of Various Lignins in Transparent Films.** The lignins prepared using various species and extraction methods were mixed with a poly(2-hydroxyethyl methacrylate) (PHEMA) solution and then cast onto quartz slides to obtain transparent films (Figures S23 and S24). For example, PHEMA containing  $\text{MWL}_{\text{CC}}$  had a peak at a longer wavelength than any other MWL (Figure S23), and PHEMA containing KL showed the highest PL intensity, with a peak at a longer wavelength than the other five lignins (Figure S24).

The analysis presented in the previous section confirmed that the environmental media affected the PL properties. To design transparent photoluminescent materials, it is necessary to clarify whether the solvent or the polymeric media has a greater influence on the PL properties. Therefore, the hydrophilic polymer (PHEMA) was compared with a hydrophobic polymer (poly(methyl methacrylate); PMMA) in the same solvent (DMF) to understand the impacts of the polymer characteristics. Figure 5 presents the normalized PL spectra of KL in PHEMA and PMMA excited at 320 nm (non-normalized data are shown in Figure S25). Furthermore, owing to its relatively low polarity, PMMA can be dissolved in both DMF and  $\text{CHCl}_3$ , and therefore, PMMA films were prepared from DMF and  $\text{CHCl}_3$  solutions to deduce the solvent's effect on the PL properties. The PHEMA and PMMA films had distinct spectral shapes and intensities, despite the fact that they contained the same lignin (KL) and solvent (DMF). This result indicated that the properties of the polymer also affected the PL spectra. Furthermore, the PMMA films prepared from DMF and  $\text{CHCl}_3$  solutions had clearly different spectra. Specifically, the PMMA film prepared from a

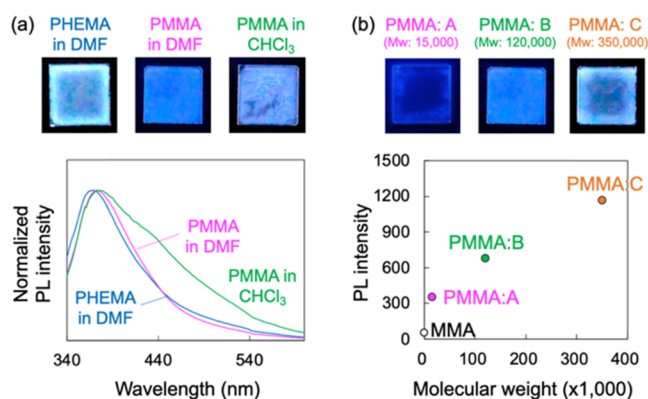


**Figure 5.** (a) Normalized PL spectra of KL in PHEMA and PMMA films prepared using DMF or  $\text{CHCl}_3$ . (b) PL intensity of KL in PMMA films with different average molecular weights (15 000, 120 000, and 350 000). The monomer (methyl methacrylate (MMA) in the liquid state) is included as a reference.

$\text{CHCl}_3$  solution exhibits PL at a longer wavelength; this behavior was consistent with the solution results presented in Figure 3.

Moreover, when films were prepared from PMMA with various molecular weights, the higher-molecular-weight polymers exhibited more intense PL (Figure 5b). The molecular weight of the polymer is closely related to its stiffness (firmness), and lignin demonstrated greater PL intensity in the stiff media (details in Figure S26). This result is consistent with the correlation between PL intensity and solvent viscosity (Figures S14–S17).

**PL Properties Depend on Species, Extraction Method, Solvent, and Polymer.** According to the PL analysis of various lignins, the PL properties depend on the taxonomical species, extraction method, solvent, and polymer used for their preparation. In other words, a variety of PL properties can be obtained by appropriately selecting those four factors. The range of colors produced in this work are plotted on a chromaticity diagram with some representative PL

spectra in Figure 6. The detailed data regarding solutions and polymers are summarized in Tables S2 and S3, respectively.

## CONCLUSIONS

In this work, the PL properties of various lignins were tuned by implementing different taxonomic species and extraction methods during their preparation. The lignins' structural differences clearly influenced their PL properties, including the emission intensity and color. Furthermore, PL quenching and a peak shift were observed in  $\text{CHCl}_3$  according to PL spectral analysis in various solvents; the potential mechanisms leading to this behavior were discussed. Characterization of the lignin in  $\text{CHCl}_3$  solution indicated that the quenching phenomenon was likely caused by the decreasing distances between aromatic moieties (luminophores) in hydrophobic solvents. Therefore, PL quenching could be controlled by modifying the proximity of luminophores. Based on this conclusion, transparent PL films were successfully prepared. In summary, a variety of PL properties were obtained by modulating the following factors: species, extraction method, solvent, and polymer. The tunability of lignin PL highlights this material's great potential as a feedstock for a wide variety of valuable materials, such as fluorescence reagents and spectral conversion agents. The results presented herein provide a basis for developing lignin-first biorefinery systems.

## ASSOCIATED CONTENT

### Supporting Information

The Supporting Information is available free of charge at <https://pubs.acs.org/doi/10.1021/acsomega.1c06104>.

Additional experimental details, materials and methods, and spectra data (PDF)

## AUTHOR INFORMATION

### Corresponding Authors

Masatsugu Takada – Graduate School of Energy Science, Kyoto University, Kyoto 606-850, Japan; [orcid.org/0000-](https://orcid.org/0000-)

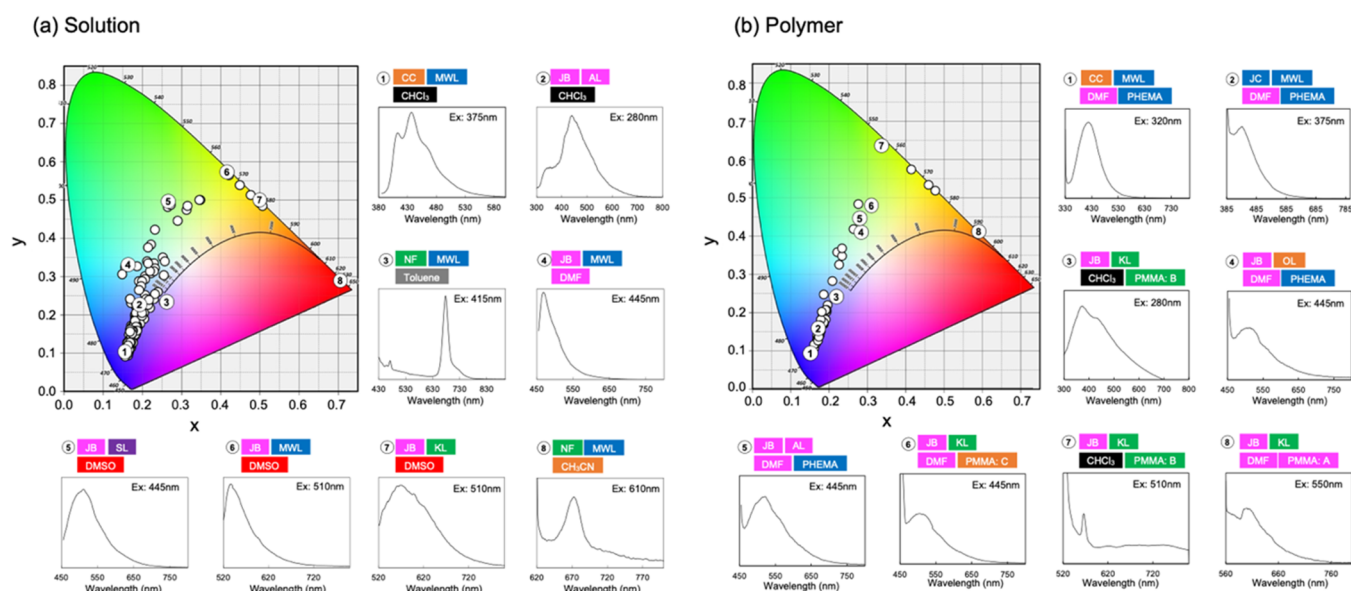


**Figure 6.** Chromaticity diagrams of lignin photoluminescence in various (a) solvents and (b) polymers obtained by selecting the species, extraction method, solvent, and polymer film.

0002-8322-3423; Phone: +81-75-753-9122;

Email: [takada.masatsugu.6n@kyoto-u.ac.jp](mailto:takada.masatsugu.6n@kyoto-u.ac.jp)

Yutaka Okazaki – Graduate School of Energy Science, Kyoto University, Kyoto 606-850, Japan; Phone: +81-75-753-9117; Email: [okazaki.yutaka.8c@kyoto-u.ac.jp](mailto:okazaki.yutaka.8c@kyoto-u.ac.jp)

## Authors

Haruo Kawamoto – Graduate School of Energy Science, Kyoto University, Kyoto 606-850, Japan

Takashi Sagawa – Graduate School of Energy Science, Kyoto University, Kyoto 606-850, Japan; [orcid.org/0000-0002-0908-0487](https://orcid.org/0000-0002-0908-0487)

Complete contact information is available at:

<https://pubs.acs.org/10.1021/acsomega.1c06104>

## Author Contributions

The manuscript was written through contributions of all authors. All authors have given approval to the final version of the manuscript.

## Notes

The authors declare no competing financial interest.

## ACKNOWLEDGMENTS

This work was supported by KAKENHI (grant nos. 20K22591 and 19K15376) and SPIRITS2020 of Kyoto University. The authors thank Dr. Mizuho Kondo from the University of Hyogo for permission to use the fluorescence lifetime measurement instrumentation.

## REFERENCES

- (1) Lora, J. H. In *Monomers, Polymers and Composites from Renewable Resources*; Belgacem, M. N.; Gandini, A., Eds.; Elsevier: Amsterdam, 2008.
- (2) Shikinaka, K.; Nakamura, M.; Otsuka, Y. Strong UV Absorption by Nanoparticulated Lignin in Polymer Films with Reinforcement of Mechanical Properties. *Polymer* **2020**, *190*, No. 122254.
- (3) Sadeghifar, H.; Ragauskas, A. Lignin as a UV Light Blocker — A Review. *Polymers* **2020**, *12*, 1134.
- (4) Chabbert, B.; Terryn, C.; Herbaut, M.; Vaidya, A.; Habrant, A.; Paës, G.; Donaldson, L. Fluorescence Techniques Can Reveal Cell Wall Organization and Predict Saccharification in Pretreated Wood Biomass. *Ind. Crops Prod.* **2018**, *123*, 84–92.
- (5) Donaldson, L. A.; Radotic, K. Fluorescence Lifetime Imaging of Lignin Autofluorescence in Normal and Compression Wood. *J. Microsc.* **2013**, *251*, 178–187.
- (6) Donaldson, L.; Radotić, K.; Kalauzi, A.; Djikanović, D.; Jeremić, M. Quantification of Compression Wood Severity in Tracheids of *Pinus radiata* D. Don Using Confocal Fluorescence Imaging and Spectral Deconvolution. *J. Struct. Biol.* **2010**, *169*, 106–115.
- (7) Xue, Y.; Wan, Z.; Ouyang, X.; Qiu, X. Lignosulfonate: A Convenient Fluorescence Resonance Energy Transfer Platform for the Construction of a Ratiometric Fluorescence PH-Sensing Probe. *J. Agric. Food Chem.* **2019**, *67*, 1044–1051.
- (8) Terryn, C.; Paës, G.; Spriet, C. FRET - SLiM on Native Autofluorescence: A Fast and Reliable Method to Study Interactions between Fluorescent Probes and Lignin in Plant Cell Wall. *Plant Methods* **2018**, *14*, No. 74.
- (9) Xue, Y.; Qiu, X.; Wu, Y.; Qian, Y.; Zhou, M.; Deng, Y.; Li, Y. Aggregation-Induced Emission: The Origin of Lignin Fluorescence. *Polym. Chem.* **2016**, *7*, 3502–3508.
- (10) Ma, Z.; Liu, C.; Niu, N.; Chen, Z.; Li, S.; Liu, S.; Li, J. Seeking Brightness from Nature: J-Aggregation-Induced Emission in Cellulolytic Enzyme Lignin Nanoparticles. *ACS Sustainable Chem. Eng.* **2018**, *6*, 3169–3175.
- (11) Xue, Y.; Qiu, X.; Ouyang, X. Insights into the Effect of Aggregation on Lignin Fluorescence and Its Application for Microstructure Analysis. *Int. J. Biol. Macromol.* **2020**, *154*, 981–988.
- (12) Konschin, H.; Franciska, S. Protolytic Dissociation of Electronically Excited Phenols Related to Lignin Part 2, Isoeugenol and Coniferyl Alcohol. *Finn. Chem. Lett.* **1974**, *5*, 46–49.
- (13) Albinsson, B.; Li, S.; Lundquist, K.; Stomberg, R. The Origin of Lignin Fluorescence. *J. Mol. Struct.* **1999**, *508*, 19–27.
- (14) Lundquist, K.; Josefsson, B.; Nyquist, G. Analysis of Lignin Products by Fluorescence Spectroscopy. *Holzforschung* **1978**, *32*, 27–32.
- (15) da Hora Machado, A. E.; De Paula, R.; Ruggiero, R.; Gardrat, C.; Castellan, A. Photophysics of Dibenzodioxocins. *J. Photochem. Photobiol., A* **2006**, *180*, 165–174.
- (16) Radotić, K.; Kalauzi, A.; Djikanović, D.; Jeremić, M.; Leblanc, R. M.; Cerović, Z. G. Component Analysis of the Fluorescence Spectra of a Lignin Model Compound. *J. Photochem. Photobiol., B* **2006**, *83*, 1–10.
- (17) Björkman, A. Studies on Finely Divided Wood. Part 1. Extraction of Lignin with Neutral Solvents. *Sven. Papperstidn.* **1956**, *59*, 477–485.
- (18) Faix, O. Fourier Transform Infrared Spectroscopy. In *Methods in Lignin Chemistry*; Lin, S. Y.; Dence, C. W., Eds.; Springer: Berlin, Heidelberg, 1992; pp 233–241.
- (19) Haidekker, M. A.; Brady, T. P.; Lichlyter, D.; Theodorakis, E. A. Effects of Solvent Polarity and Solvent Viscosity on the Fluorescent Properties of Molecular Rotors and Related Probes. *Bioorg. Chem.* **2005**, *33*, 415–425.
- (20) Argyropoulos, D. S. Salient Reactions in Lignin during Pulping and Oxygen Bleaching. *J. Pulp Pap. Sci.* **2003**, *29*, 308–313.